Front. Optoelectron. 2012, 5(2): 231–236
DOI 10.1007/s12200-012-0251-4

RESEARCH ARTICLE

A novel Stokes parameters coding scheme for free-space coherent optical communication

Qing WAN, Chunhui HUANG (✉)

College of Physics and Information Engineering, Fuzhou University, Fuzhou 350002, China

Abstract This paper proposes a novel continuous variable coherent optical communication mode. In this mode, two quadrature Stokes parameters are regarded as observed physical quantity, and single linearly polarized component is used as carrier wave. At the sending end, electro-optical amplitude modulator (EOM) of 45° azimuth is used to indirectly complete the linear modulation of S_2 component, and S_3 component is changed by continuously rotating a half-wave plate (HWP). The receiving end adopts the mode of Q-Q-H wave plate are rotated to select the component of measured S_2 or S_3. The circuit of balance homodyne detection is designed, and the detection system is built by combination with LabVIEW to complete signal demodulation. New optical path scheme is verified by both theory and experiment.

Keywords continuous variable coherent optical, Stokes parameters, electro-optical modulator, balance homodyne detection

1 Introduction

Quantum cryptography communication is a promising technology using the quantum natures of light to achieve the security in telecommunication [1]. Like single photon as quantum key distribution (QKD), continuous variable coherent optical beam can be used to quantum cryptography communication. Compared with the single photon QKD scheme, continuous variable coherent schemes are more attractive because of their high efficiency and compatibility [2]. The continuous variable quantum cryptography setups can easily encode and transmit. Gaussian cryptographic protocols for coherent states have shown its potential on the applications of quantum communication. These protocols are robust due to it can overcome the quantum channel noise.

In the continuous variables coherent optical communication systems, the signal light was injected into a Mach-Zehnder (M-Z) interferometer. In the M-Z interferometer, one beam linearly polarized light was divided into two quadrature coherent components and propagate along the two branches [3]. One of them can be used as the local oscillator (LO), and the amplitude and phase of the other one is Gaussian modulated to carry information. In the output of the M-Z interferometer, two components are coupled for detection. According to the Heisenberg uncertainty principle and quantum no-cloning theorem [4], the two components of coherent light can guarantee the security of signal transmission. In the M-Z interferometer based free-space transmission schemes, the optical coupling and phase synchronization is unstable in the receiver of the systems. Elser et al. [5] proposed a single-mode spatial optical signal transmission scheme to simplify the setup of the continuous variables coherent optical communication scheme. But this scheme cannot achieve the base selection for the Stokes components $\hat{S}_2$ and $\hat{S}_3$ at the receiver end, which is required by the applications of quantum cryptography communication.

In this paper, we demonstrated a scheme using Stokes parameter coding for the continuous variable coherent optical communication scheme to stabilize optical coupling and phase synchronization. The corresponding experimental setup is also demonstrated, which uses SU(2) converter in the detector setup to achieve the base selection.

2 Theoretical analyses

The state of polarization (SOP) of the input light can be presented by Jones matrix as follows [6–8]:

Received January 7, 2012; accepted February 8, 2012

E-mail: hchuang@fzu.edu.cn

$$\boldsymbol{E} = \begin{pmatrix} E_x & E_y \end{pmatrix}^{\mathrm{T}}. \tag{1}$$

When passing through the polarizer and two polarized beam splitters (PBS), the light is transformed to a pure horizontal polarization. The horizontal polarized light is presented as

$$\boldsymbol{E}_1 = \begin{pmatrix} E_x & 0 \end{pmatrix}^{\mathrm{T}}. \tag{2}$$

In this scheme, an electro-optical amplitude modulator (EOM) is used to adjust the phase delay of the horizontal polarized light. Here, electro-optical crystal acts as a phase delay adjustable wave plate, which can be written as follows [9]:

$$\boldsymbol{E}_{\mathrm{eom}} = \begin{pmatrix} \mathrm{e}^{-\mathrm{i}(\tau/2)}\cos^2\varphi + \mathrm{e}^{\mathrm{i}(\tau/2)}\sin^2\varphi & -\mathrm{i}\sin(\tau/2)\sin(2\varphi) \\ -\mathrm{i}\sin(\tau/2)\sin(2\varphi) & \mathrm{e}^{-\mathrm{i}(\tau/2)}\sin^2\varphi + \mathrm{e}^{\mathrm{i}(\tau/2)}\cos^2\varphi \end{pmatrix}, \tag{3}$$

where φ is the angle between the crystal axis and the horizontal direction; τ is the phase delay of the crystal. After passing through the EOM, the Jones matrix of the signal light becomes

$$\boldsymbol{E}_{\mathrm{out}} = E_x \begin{pmatrix} \mathrm{e}^{-\mathrm{i}(\tau/2)}\cos^2\varphi + e^{\mathrm{i}(\tau/2)}\sin^2\varphi \\ -\mathrm{i}\sin(\tau/2)\sin(2\varphi) \end{pmatrix}. \tag{4}$$

As we know, the SOP of light can be represented by Stokes parameters, which can be mapped to a Poincaré sphere face as shown in Fig. 1.

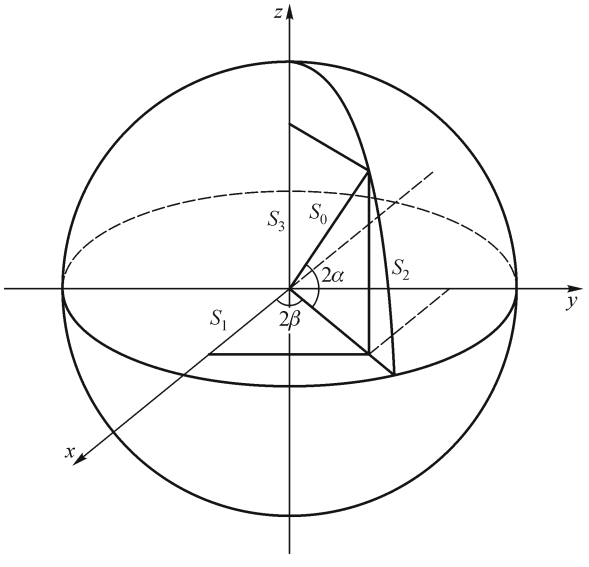

Fig. 1 Poincaré sphere

So that one point on the sphere face present one polarization states. As shown in Fig. 1 [10], the following formulas can be written.

$$S_0 = \sqrt{S_1^2 + S_2^2 + S_3^2},$$

$$S_1 = S_0\cos(2\alpha)\cos(2\beta),$$

$$S_2 = S_0\cos(2\alpha)\sin(2\beta),$$

$$S_3 = S_0\sin(2\alpha). \tag{5}$$

In our proposed Stokes parameter coding schemes, S_2 or S_3 can be encoded by modulating angels of α and β, through EOM and magneto-optical modulation (MOM).

Now, the Stokes components of signal light after the EOM can be seen as [11]

$$S_2 = \hat{\boldsymbol{E}}_{\mathrm{EOM}}\boldsymbol{P}_3\boldsymbol{E}_{\mathrm{EOM}},$$

$$S_3 = \hat{\boldsymbol{E}}_{\mathrm{EOM}}\boldsymbol{P}_4\boldsymbol{E}_{\mathrm{EOM}}, \tag{6}$$

where $\boldsymbol{P}_3$, $\boldsymbol{P}_4$ are the sandwich matrixes, which are

$$\boldsymbol{P}_3 = \begin{bmatrix} 0 & 1 \\ 1 & 0 \end{bmatrix}, \ \boldsymbol{P}_4 = \begin{bmatrix} 0 & \mathrm{i} \\ -\mathrm{i} & 0 \end{bmatrix}. \tag{7}$$

So S_2 and S_3 can be described as follows:

$$S_2 = -E_x^2\sin^2(\tau/2)\sin 4\varphi,$$

$$S_3 = E_x^2\sin(2\varphi)\sin\tau. \tag{8}$$

Here, it is noted that when $\varphi = 45^\circ$, we can set S_2 component to zero and modulate the S_3 component independently. Then, we will get $S_3 = E_x^2\sin\tau$. The experimental setup is shown in Fig. 2.

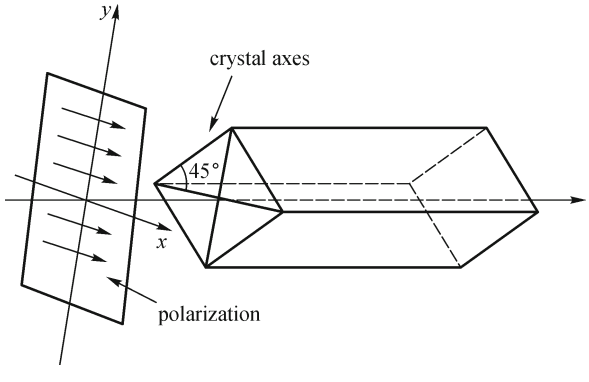

Fig. 2 Position of electro-optic crystal

Taking $\varphi = 45^\circ$ into Eq. (8), the SOP of the signal after EOM can be derived as

$$\boldsymbol{E}_{\mathrm{out}} = \frac{1}{2}E_0 \begin{pmatrix} \cos(\tau/2) \\ -\mathrm{i}\sin(\tau/2) \end{pmatrix}. \tag{9}$$

According to Eq. (9), when τ is small, the intensity of the

horizontal component will be much larger than that of the vertical one. In our scheme, we use the stronger horizontal polarized component as the LO light, and use the vertical component as the signal light. The signal and the LO light were then transmitted along on a single spatial transmission mode.

After the EOM, S_2 components can be modulated by a MOM to carry the signal.

The simulation shows that when half-wave plate (HWP) rotates on the azimuth, the S_2 component of polar light will be changed such as the MOM. When modulating the signal, we consider the delay between the EOM and HWP. Thus the signal and LO are synchronized at the output of HWP. Since the Jones matrix of HWP is [12]

$$\boldsymbol{E}_{\mathrm{H}} = -\mathrm{i}\begin{pmatrix} \cos(2\phi) & \sin(2\phi) \\ \sin(2\phi) & -\cos(2\phi) \end{pmatrix}, \tag{10}$$

where ϕ presents the included angle between the crystal axis and horizontal component of signal light, the optical signal after the MOM can be written as

$$\boldsymbol{E}_{\mathrm{out2}} = \frac{1}{2}E_x\begin{pmatrix} -\mathrm{i}\cos(2\phi)\cos(\tau/2) - \sin(2\phi)\sin(\tau/2) \\ -\mathrm{i}\sin(2\phi)\cos(\tau/2) + \cos(2\phi)\sin(\tau/2) \end{pmatrix}. \tag{11}$$

The Stokes components of the output light are

$$S_2 = \frac{1}{4}E_x^2\cos\tau\sin(4\phi), \tag{12}$$

$$S_3 = \frac{1}{4}E_x^2\sin\tau. \tag{13}$$

According to Eq. (12), when the value of τ is fixed, we can modulate the S_2 by changing the angle ϕ of MOM. Equation (13) indicates that the MOM will not affect the value of S_3.

3 Experiments

3.1 Optical path design

Based on Section 2, we design a free space continuous variables coherent optical communication setup, which is shown in Fig. 3. At Alice end, a light beam at 808 nm was focused by a convex with a focus length of 8.5 mm and passes through an isolator. Then, the horizontal polarizer and two PBS ware used to convert this light into the horizontal polarization status (E_1). After that, we used an EOM (New Focus 4102M) encodes the S_3 component. Here, we rotated a HWP to control the S_2 component, which simulates the function of a MOM.

At the Bob end, the measurement base is first selected by a Q-Q-H SU(2) convert box which composes one HWP and two quarter-wave plates (QWP). Then, a PBS splits the light into a horizontal polarized component (E_2) and a vertical polarized component (E_3) for detection. A balance homodyne detection circuit was used to detect the optical signal for further digital signal processing using LabVIEW [13].

3.2 Stokes parameters detection system

At the detection end, the measurement base is selected by rotating the Q-Q-H wave plate. $\hat{a}_x$, $\hat{a}_y$ are set as the coherent polarization status of input light, and $\hat{c}_x$, $\hat{c}_y$ as the coherent polarization status of output light. The detecting optical path is shown in Fig. 4.

Since Stokes component follows the following:

$$\begin{aligned} S_2 &= \left\langle a_x^{\dagger}\, a_y \right\rangle + \left\langle a_y^{\dagger}\, a_x \right\rangle, \\ S_3 &= \mathrm{i}\left(\left\langle a_y^{\dagger}\, a_x \right\rangle - \left\langle a_x^{\dagger}\, a_y \right\rangle\right). \end{aligned} \tag{14}$$

The homodyne detection light density is

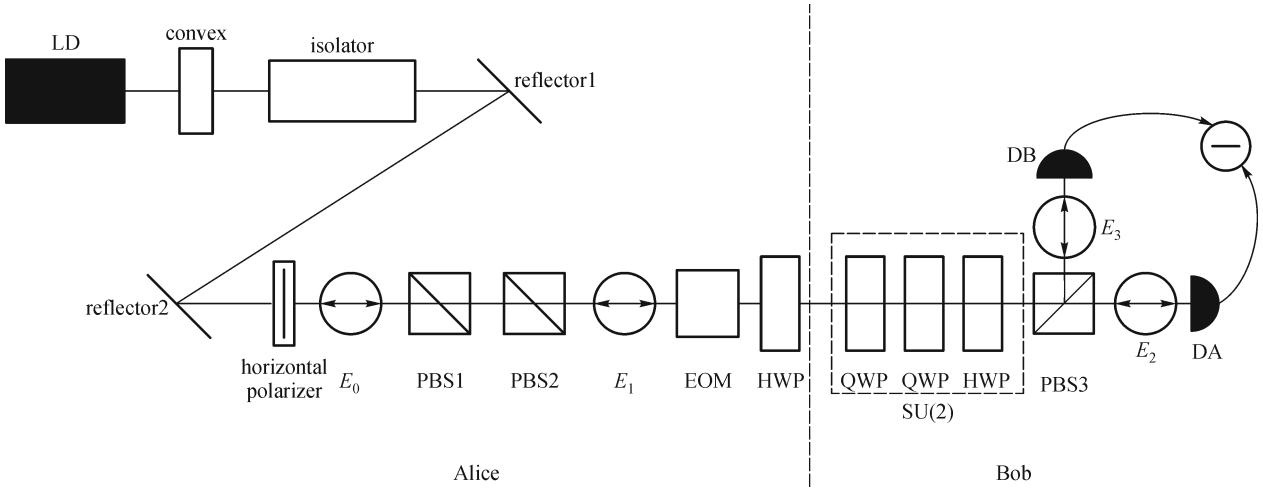

Fig. 3 Integrated optical path structure

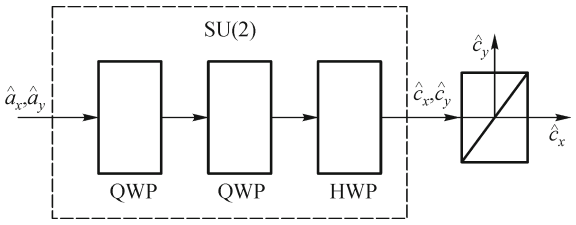

Fig. 4 SU(2) convert box

$$I = \left\langle c_y^{\dagger}\, c_x \right\rangle - \left\langle c_x^{\dagger}\, c_y \right\rangle. \tag{15}$$

The SU(2) convert box can be regarded as a Jones matrix. The output $\boldsymbol{E}_{\mathrm{su}}$ is described as

$$\boldsymbol{E}_{\mathrm{su}} = \boldsymbol{E}_{\mathrm{Q}}\boldsymbol{E}_{\mathrm{Q}}\boldsymbol{E}_{\mathrm{H}}, \tag{16}$$

where $\boldsymbol{E}_{\mathrm{Q}}$ and $\boldsymbol{E}_{\mathrm{H}}$ present the Jones matrixes of QWP and HWP, respectively. If the crystal axes of three wave plates set of particular angles different angles with the horizontal direction, respectively, Eq. (16) will satisfy the following equations:

$$I = S_2,\ \boldsymbol{E}_{\mathrm{su}} = \frac{\sqrt{2}}{2}\begin{pmatrix} 1 & 1 \\ -1 & 1 \end{pmatrix}, \tag{17}$$

$$I = S_3,\ \boldsymbol{E}_{\mathrm{su}} = \frac{\sqrt{2}}{2}\begin{pmatrix} 1 & \mathrm{i} \\ \mathrm{i} & 1 \end{pmatrix}. \tag{18}$$

The angles between the crystal axis and horizontal direction of three wave plates Q-Q-H set as α, β, ϕ, respectively.

$$\alpha = 0,\ \beta = 0,\ \varphi = -\frac{3}{8}\pi,\ \text{measure } S_2 \text{ component;}$$

$$\alpha = 0,\ \beta = -\frac{1}{4}\pi,\ \phi = -\frac{1}{8}\pi,\ \text{measure } S_3 \text{ component.}$$

From selecting the measurement base, the balance homodyne detection is implemented [14,15].

In Eq. (13), S_3 parameter is a sine function of τ, here $\tau = \frac{\pi}{V_\pi}V$, and V is the modulation voltage of EOM. The result of sine relationship between S_3 and V is shown in Fig. 5, where x-axis and y-axis present the drive voltage V and S_3 parameter, respectively. The modulation voltage V of the electro-optical crystal is a 1.6 MHz sinusoidal oscillatory wave with a V_0 direct current (DC) bias voltage. It can be written as

$$V = V_0 + V_x\sin(\omega t), \tag{19}$$

where ω is the frequency of sine wave. V_x is the input drive voltage of EOM.

According to Eqs. (13) and (19), the relationship between S_3 and V is described as follows:

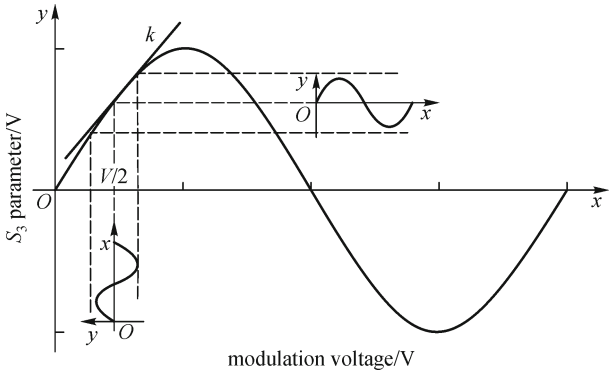

Fig. 5 Relationship between EOM voltage and S_3 parameter

$$S_3 = \frac{1}{4}E_x\sin\frac{\pi}{V_\pi}[V_0 + V_x\sin(\omega t)]. \tag{20}$$

When the change of V_x is fairly small,

$$S_3 \approx \frac{k}{4}E_x\frac{\pi}{V_\pi}[V_0 + V_x\sin(\omega t)]. \tag{21}$$

Since $\frac{k}{4}E_x\frac{\pi}{V_\pi}$ is a constant, let $M = \frac{k}{4}E_x\frac{\pi}{V_\pi}$, Eq. (21) is simplified as follows:

$$S_3 \approx M[V_0 + V_x\sin(\omega t)] = MV_0 + MV_x\sin(\omega t). \tag{22}$$

When the detection signal passes through the bandpass filter at the end of the detection circuit, the DC signal is filtered, and then

$$S_3 - MV_0 = MV_x\sin(\omega t). \tag{23}$$

4 Results and discussion

When the random selection measurement base is S_2, the relative between the horizontal azimuth ϕ of HWP and the value of S_2 component can be described as $S_2 = \frac{1}{4}E_x^2\cos\tau\sin 4\phi$. The corresponding measurement results are shown in Fig. 6.

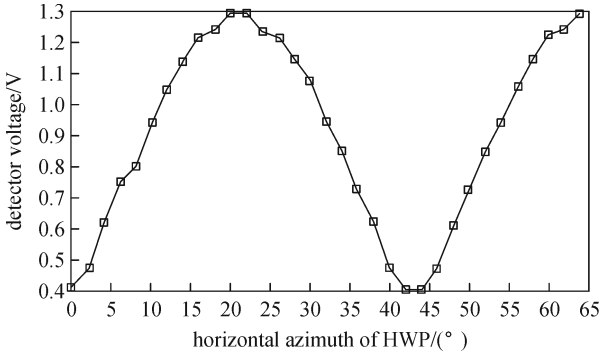

Fig. 6 Relationship between HWP ϕ and S_2

As discussed in Section 3.2, in Eq. (23), we note that the V_x is not linearly relative to the S_3. Thus, we carefully choose a linear operation point of EOM according to the relationship as shown in Fig. 5. To find the linear operation point, we measured the relationship between the detective voltage of S_3 and the driving voltage of EOM. According to the measurement, we set the operation point at 2 V.

Then, we modulate the EOM by using a random code at a bit rate of 1.6 MHz which has 16 equal parts and follows the Gaussian distribution. The length of the random code is 10^4 bits. At the receiver, the signal is linearly demodulated. Figure 7 is the probability distributions of the demodulation signal at different part, which follow the Gaussian distribution.

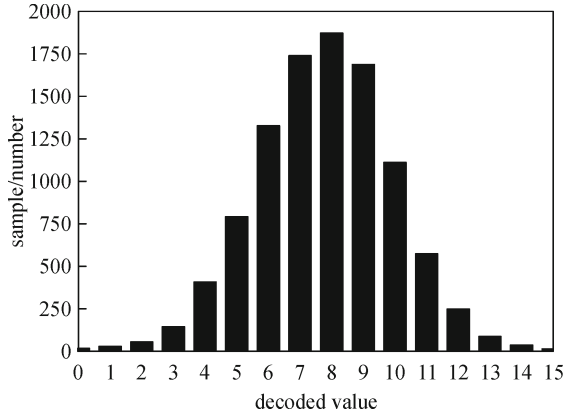

Fig. 7 Gaussian distribution of S_3 demodulation signal

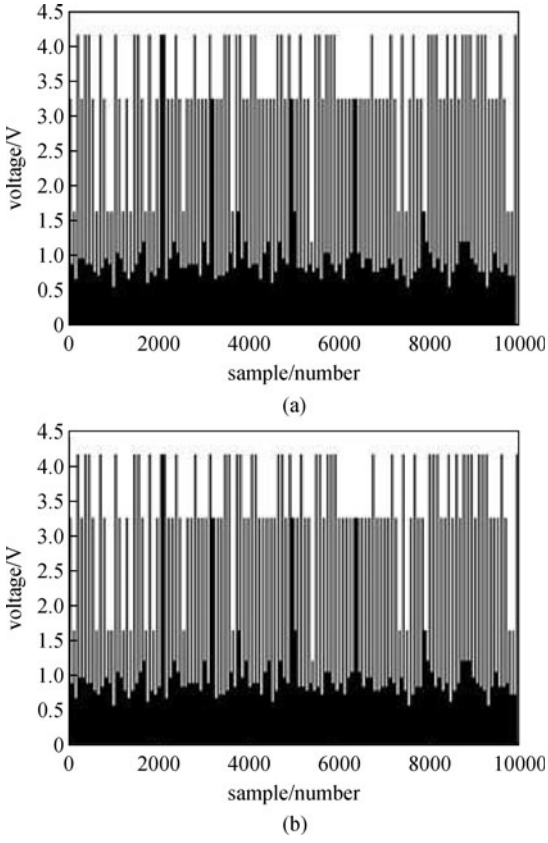

Fig. 8 Error code analysis of S_3 acquisition signal. (a) Coding value; (b) decoding value

Figure 8 shows the input and the output results. We also measure the bit error rate using the array indexing tool in LabVIEW. For 10^4 samples, the sending-to-receiving bit error rate is measured and lower than 10^{-4}, which indicates that if a linearly modulated operation point can be properly choose in the EOM, the S_3 component can be demodulated in our proposed receiver setup.

At the detection end, if we randomly rotate the SU(2) convert box to modulate the signal and singal has quantum properties, then the commutators of S_2 and S_3 components follow the uncertainty relations [16]:

$$\Delta\hat{S}_2 \cdot \Delta\hat{S}_3 \geqslant \left|\langle \hat{S}_1 \rangle\right|. \tag{24}$$

Equation (24) indicates if one Stokes operator is nonzero, the other two Stokes operators cannot be simultaneously measured with certainty because Heisenberg uncertainty principle and quantum no-cloning theorem. According to the Heisenberg uncertainty principle, the quantum broadening effect makes a potential eavesdropper cannot accurately measure the values of S_2 and S_3 components. Thus the security of the communication is guaranteed. However, we can still select two groups of components ($\hat{S}_2$ and $\hat{S}_3$) to carry the signal by using the EOM and MOM. Thus in the receiver, we can decode the information by using the relationship of $S_2 = \langle \hat{S}_2 \rangle$ and $S_3 = \langle \hat{S}_3 \rangle$.

5 Conclusions

In this paper, we proposed a scheme using Stokes parameter coding for a spatial continuous variables coherent optical communication scheme to stabilize optical coupling and phase synchronization. In the receiver, we also demonstrated that an SU(2) convert box can be used to achieve the base selection of the S_2 or S_3 components. Our experimental results also indicate if the S_3 component can be linearly modulated by properly choosing the operation point of EOM, the Stokes parameters can be demodulated in our proposed receiver setup. This scheme resolves the problem that the coherence is hard to be guaranteed in the M-Z interferometer optical path, and it has great advantages in continuous variable coherent optical communication.

Acknowledgements This work was supported by the National Natural Science Foundation of China (Grant No. 61177072).

References

1. Zheng G H. Quantum Cryptography. Beijing: Science Press, 2006, 15–40 (in Chinese)
2. Ma R L. Quantum Cryptography Communication. Beijing: Science Press, 2006, 104–118 (in Chinese)
3. Grosshans F, Van Assche G, Wenger J, Brouri R, Cerf N J, Grangier P. Quantum key distribution using gaussian-modulated coherent states. Nature, 2003, 421(6920): 238–241
4. Shu X Q, Guo G C. Quantum communication and quantum computation. Chinese Journal of Quantum Electronics, 2004, 21(6): 706–719 (in Chinese)
5. Elser D, Bartley T, Heim B, Wittmann C, Sych D, Leuch G. Feasibility of free space quantum key distribution with coherent polarization states. New Journal of Physics, 2009, 11(4): 045014
6. Korolkova N, Leuchs G, Loudon R, Raiph T C, Silberhorn C. Polarization squeezing and continuous variable polarization entanglement. Physical Review A, 2002, 65(5): 052306
7. Leonhardt U. Measuring the Quantum State of Light. Cambridge: Cambridge University Press, 1997, 144–170
8. Tang Z L, Li M, Wei Z J, Lu F, Liao C J, Liu S H. The quantum key distribution system based on polarization states produced by phase modulation. Acta Physica Sinica, 2005, 54(6): 2534–2539
9. Yariv A, Yeh P. Optical Electronics in Modern Communictaions. 6th ed. Oxford: Oxford University Press, 2007, 36–45
10. Chen W B, Gu P F. Using Stokes vector express polarized light and application. Optical Instruments, 2006, 26(5): 42–46 (in Chinese)
11. Wei Y D, Tang Z L, Liu X B, Liao C J, Liu H H. Study on sending after verify scheme in quantum channel for quantum key distribution system based on polarization coding. Acta Photonica Sinica, 2009, 38(7): 1852–1857
12. Liao Y B. Polarization Optics. Beijing: Science Press, 2003, 49–57 (in Chinese)
13. Travis J, Kring J. LabVIEW for Everyone: Graphical Programming Made Easy and Fun. 3rd ed. Beijing: Publishing House of Electronics Industry, 2008, 55–87 (in Chinese)
14. Chen C, Huang C H. Improved version of coherent light detection system design. Laser & Infrared, 2008, 38(6): 580–582 (in Chinese)
15. Chen S H, Huang C H. Application of LabVIEW in homodyne coherent light detection system. Chinese Journal of Quantum Electrons, 2009, 26(3): 371–375 (in Chinese)
16. Dong C H. The quantum description of polarization states of light and its evolutions in the processes of interaction with atoms. Acta Physica Sinica, 2005, 54(2): 687–694 (in Chinese)